Effect of Cosolvents on the Adsorption of Peptides at the Solid−Liquid Interface

Amol Mungikar and Daniel Forciniti*

Chemical and Biological Engineering Department, University of Missouri−Rolla, Rolla, Missouri 65409

Received August 28, 2005; Revised Manuscript Received November 5, 2005

The adsorption of a peptide at solid surfaces is the result of a complex interplay of interactions between the peptide, solvent, and surface. In this work, Monte Carlo simulations were performed to evaluate the effect of the solvent hydrogen bonding ability on the adsorption of the peptide ASP^1-ASP^2-ILE^3-ILE^4-ASP^5-ASP^6-ILE^7-ILE^8 at a charged surface consisting of CH_2 atoms with a fixed lattice arrangement. Various water−alcohol mixtures were used as solvent because alcohols are known to alter the dielectric constant, hydrophobicity, and hydrogen bonding capacity of water. Solvent−solvent, solvent−surface, solvent−peptide, and peptide−surface interactions were studied independently and correlated with the observed peptide behavior at the solvent−surface interface. We concluded that the behavior (and orientation) of the peptide at the surface is directly related to changes in water−water hydrogen bonding properties in water−alcohol mixtures. In the presence of increasing concentrations of methanol, the strength of solvent−peptide and solvent−surface interactions was reduced, and as a result, a stronger interaction between the peptide and the surface was observed. Stronger solvent−peptide and solvent−surface interactions were responsible for a weaker interaction of the peptide with the surface in the presence of increasing concentrations of glycerol. These results suggest that by changing solvent conditions it is possible to finely tune the orientation of a macromolecule at solid/liquid interfaces.

Introduction

A fundamental understanding of protein behavior at solid−liquid interfaces is important to improve our knowledge of various natural and synthetic processes. A few examples where protein adsorption at the solid−liquid interface may play an important role are found in blood coagulation, artificial kidney failure, biomedical microdevices, self-assembling microelectromechanical systems, protein-based microarrays, design and fabrication of biosensors/biomaterials, and filtration systems in bioseparation processes. Several reviews are available describing various methods to study protein adsorption, and some highlight the importance of developing both experimental and theoretical models simultaneously.[1−5] In this paper, we present a computer simulation approach to study the adsorption of peptides at solid/liquid interfaces. Solvent−solvent, solvent−protein, solvent−surface, and protein−surface interactions can be individually studied at the molecular level (a type of study that escapes the capabilities of current experimental techniques). Simulations can be of immense importance in this aspect because the properties of the protein, solvent, and surface can be easily (and systematically) varied within a reasonable period of time.

The control of the amount of protein adsorbed and of the orientation and conformation of the protein at the surface are critical in many applications. For example, the sensitivity of enzyme linked immunosorbent assays depends strongly on the appropriate control of the orientation of the immobilized antibody. Almost all of the biomanufacturing activities, biosensor applications, and chromatographic separation techniques require minimal (uncontrolled) protein adsorption because of its undesirable effects on the process's efficiency. The preferred choice to modulate the orientation of a protein at a surface has been to change the surface chemistry.[6−9] For example, Seigers et al.[6] have reported that self-assembled monolayers of dendritic polyglycerol derivatives on gold surface resist adsorption of proteins. Lasseter et al.[7] have demonstrated that the orientation and amount of protein adsorbed on silicon and diamond surfaces can be controlled by modifying the surface with short ethylene glycol oligomers by direct covalent functionalization. Fang and Szleifer[8] have theoretically demonstrated (using a mean-field approach) that it would be possible to reduce protein adsorption by coating the surface of the adsorbent with model polymers mimicking poly(ethylene) oxide. They concluded that protein adsorption is very sensitive to the type of surface modifier. Lee et al.[9] reported differences in mean molecular orientation in monolayer and submonolayer films of both myoglobin and cytochrome *c* adsorbed on hydrophilic and hydrophobic glass surfaces. They argued that the observed behavior is due to different functionalities of the proteins and the surfaces.

Protein adsorption can be controlled by changing the composition of the solvent instead of altering the surface chemistry. This is possible because a change in solvent composition may change the interaction potential between the protein and the surface and between proteins. For example, the addition of alcohols, such as methanol or glycerol, is expected to change the dielectric constant, hydrogen bonding capability, and hydrophobicity of water. The change in dielectric constant affects the electrostatic interactions originated by charge distributions in the protein/peptide, surface, and solvent. Along with these changes in electrostatic interactions, changes in hydrogen bonding capabilities and in hydrophobicities are expected to induce differences in intermolecular interactions among the protein/peptide, the solvent, and the surface. There are few reports[10−12] describing the effect of the addition of cosolvents such as sorbitol, glycerol, and methanol on protein adsorption. For example, Berna et al.[10] studied the effects of sorbitol and glycerol on the adsorption and desorption of serum proteins on an amphiphilic mercaptomethylene pyridine-derivatized agarose gel. They found that sorbitol promoted protein adsorption while glycerol disrupted protein interactions and thus they suggested their use instead

* To whom correspondence should be addressed. Tel: 01-573-341-4427. E-mail: forcinit@umr.edu.

10.1021/bm050619z CCC: $33.50
Published on Web 12/10/2005

of water-structuring salts during the adsorption phase. Song and Forciniti[11] found that the adsorption of HSA on polystyrene was sensitive to both pH and type of solvent, whereas pH and solvent showed little effect on IgG adsorption on polystyrene. For HSA, they reported reduced adsorption in methanol at pH 6.9 and 9.0 and enhanced adsorption in 15% glycerol at pH 4.8 (with end-on orientation). They observed no changes in the adsorption of IgG in methanol but enhanced adsorption in 15% glycerol. Tilton et al.[12] used methanol and glycerol as cosolvents to study the role of hydrophobic interactions in the adsorption of ribonuclease A on polystyrene. They found that there was an enhanced adsorption rate of ribonuclease A on polystyrene in the presence of 33% glycerol, whereas it was reduced in the presence of 25% and 50% methanol. They concluded that, by manipulating the magnitude of the hydrophobic interaction, the adsorption mechanism can be altered through both fluid-phase transport and protein binding at the interface. Because of the complex nature of such systems, it is difficult to experimentally determine the exact orientation (and any possible surface-induced conformational change) of the adsorbed protein. Moreover, it is particularly challenging to systematically study the effect of solvent composition on the orientation of the macromolecule at the solid/liquid interface; in all of the above examples, only a few solvent compositions have been explored. Molecular simulations can help in the understanding of the phenomenon and to provide experimentalists with a few selected experimental conditions under which it would be possible to orient the peptide in a preferred direction. It is important to recognize that by changing the composition of the solvent it is possible to continuously change those properties that are expected to affect the orientation of the macromolecule at the interface.

One possible drawback of the use of solvents to modulate the orientation of a macromolecule at an interface is to disrupt the native conformation of the macromolecule. Computer simulations and spectroscopic studies have shown that the stability of the protein or peptide in bulk in the presence of alcohols depends on the type and concentration of alcohol and on the intrinsic stability of the protein. Other factors must be taken into account when, in addition to a solvent, the macromolecule is exposed to an interface. The properties of the sorbent material, the solution, the structural characteristics of the protein, and the degree of surface coverage are known to play an important role in determining the conformational stability of the protein at the solid surface. For example, it is known that proteins undergo significant conformational changes at hydrophobic surfaces such that nonpolar amino acids interact preferentially with the surface. This induces strong interfacial interactions and irreversible adsorption. It is not clear whether the addition of moderate amounts of a "denaturing" solvent such as methanol would increase the magnitude of those conformational changes. Electrostatic interactions dominate the interfacial interactions on hydrophilic or charged surfaces, and adsorption is more reversible.[13,14] Although the tendency to retain the native conformation strongly depends on the inherent structural stability of the protein in the solution, some structural rearrangement at the interface is possible to maximize the availability of the amino acid side chains that are electrostatically complementary to the surface.[15] Obviously, these electrostatic complementarities will be also affected by a change in solvent composition.

In the direction of the experimental work done by Song and Forciniti,[11] we have used Monte Carlo simulations to study the effect of the addition of alcohols on the adsorption of a model 8-residue peptide onto a charged solid surface while keeping constant the properties of the peptide and the surface. The use of short peptides (rather than complete proteins)[15] is attractive because by using a "simpler" adsorbate the interpretation of the results is simplified, and therefore, more general conclusions can be reached. Methanol and glycerol at various concentrations were used as cosolvents. The change in dielectric properties of the alcohol−water mixtures was integrated in the simulations by explicit treatment of the solvent. Hydrogen bonding network, and hydrophobicity,[16−17] solvent−solvent, solvent−peptide, solvent−surface, and peptide−surface interactions were individually studied to fully understand the effect of solvent on electrostatic interactions. By manipulating the properties of the solvent, the adsorption process is "forced" to respond to changes in the interactions of the solvent with the peptide and the surface, whereas all of the adsorbent properties remain unaltered. This overcomes the uncertainties associated with the inadequate control of surface chemistry in studying the adsorption mechanism and it allows a "continuous" variation in the driven forces for adsorption. As far as we know, nobody has attempted to model solvent/cosolvent effects in peptide (or protein) adsorption using Monte Carlo simulations.

Peptide

The model 8-residue peptide is a peptide of aspartic acid (ASP) and isoleucine (ILE). Aspartic acid is a polar amino acid that carries a negative charge at pH 7, whereas isoleucine is a nonpolar amino acid.[18] The sequence of the amino acids in the 8-residue peptide was (N) ASP^1-ASP^2-ILE^3-ILE^4-ASP^5-ASP^6-ILE^7-ILE^8(C). The superscripts represent the sequential order of the residues in the peptide chain, which are used to identify these residues later on. The peptide has an energy minimized α-helix conformation that was generated by the molecular modeling software ALCHEMY (Tripos Inc., St Louis, MO). A RASMOL generated ribbons view of the α-helix conformation of this model 8-residue peptide is shown in our earlier work.[15] The peptide has a fixed bond length and bond angle but has torsional flexibility. The torsion angles of the peptide are Φ (rotation about $N-C^\alpha$) $= -58°$ and Ψ (rotation about $C^\alpha - C$) $= -47°$. All peptide atoms are treated explicitly except for the methyl groups, CH_X ($X = 1-3$), which are treated as united atoms. The peptide has a volume of 797.3 $Å^3$ and an overall charge of −4e.

Methods

The interaction potential used for any pair of atoms, whether solute or solvent, was a spherically symmetric Lennard-Jones (LJ) plus a Coulomb term

$$u_{\alpha\beta} = \left\{\frac{A_{\alpha\beta}}{r}\right\}^{12} - \left\{\frac{C_{\alpha\beta}}{r}\right\}^{6} + \frac{e^2 q_\alpha q_\beta}{4\pi\epsilon_0}\left\{\frac{1}{r}\right\} \qquad (1)$$

where $A_{\alpha\beta}$ and $C_{\alpha\beta}$ are the repulsive and dispersive coefficients of the LJ potential, r is the distance between atoms α and β, q_α and q_β are the partial charges on atoms α and β respectively, and ϵ_0 is the permittivity.

The conformational energy of the peptides was calculated as the sum of LJ, electrostatics, and nonbonded torsional energies. A three term Fourier series was used to represent the intrinsic torsional energy[19]

$$E_{\text{torsion}} = \left(\frac{V_1}{2}\right)(1 + \cos\theta) + \left(\frac{V_2}{2}\right)(1 - \cos 2\theta) + \left(\frac{V_3}{2}\right)(1 + \cos 3\theta) \qquad (2)$$

Table 1. Coefficients in Equation 2

for ϕ (rotation about N−C^a)		for Ψ (rotation about C^a−C)	
parameter	value	parameter	value
V_1	0.000	V_1	1.849
V_2	0.000	V_2	0.950
V_3	1.498	V_3	0.840

Table 2. (a) Effective LJ Parameters for the Methanol Model[21] and (b) Effective Charge and Geometrical Parameters for the Methanol Model[21]

(a)

A_{OO} (Å-K$^{1/12}$)	C_{OO} (Å-K$^{1/6}$)	$A_{CH_3CH_3}$ (Å-K$^{1/12}$)	$C_{CH_3CH_3}$ (Å-K$^{1/6}$)	A_{OH} (Å-K$^{1/12}$)	A_{CH_3H} (Å-K$^{1/12}$)
4.993	8.119	6.241	10.319	0.000	0.000

(b)

q_O (e)	q_{CH_3} (e)	q_H (e)	L_{OCH_3} (Å)	L_{OH} (Å)	θ_{HOCH_3} (°)
−0.574	+0.176	+0.398	1.430	1.000	108.48

where θ is the torsion angle (either ϕ (rotation about N−C$^\alpha$) or Ψ (rotation about C−C$^\alpha$)), the coefficients in eq 2: V_1, V_2, and V_3 are given in Table 1.

A simple point charge (SPC) model[20] was used for water. The model developed by van Gunsteren et al.[21] was used for methanol (the parameters are listed in Table 2, parts a and b), and a model introduced by Root and Stillinger[22] was used for glycerol, with all parameters listed in Table 3, parts a and b. The effective pair potential parameters and partial charges for the peptide atoms and surface atoms are listed in Table 4. The LJ potential parameters between unlike charges were calculated using the geometric mean combination rule

$$A_{ij} = \sqrt{A_{ii}A_{jj}}$$
$$C_{ij} = \sqrt{C_{ii}C_{jj}} \qquad (3)$$

Two surfaces of the same charge density but opposite sign were placed at the two ends of the simulation box. The surface was modeled to mimic a solid surface in which all of the atoms have LJ parameters $\sigma = 3.964$ Å and $\epsilon = 70.49$ K. The same charge density of 0.02711e/Å^2 was used for both methanol−water and glycerol−water systems. This surface is insensitive to the solvent environment. The LJ parameters correspond to a united CH_2 atom. A total of 226 atoms in four layers were arranged in a face centered cubic (FCC) 111 crystal lattice structure.[15] Four sodium ions were included to maintain electroneutrality in the system. Sodium ions preferred to stay in the vicinity of the negatively charged surface and as a result did not play a direct role in peptide adsorption at the positively charged surface. We used periodic boundary conditions in the X and Y directions only, and thus, the presence of the charged surface at the two ends of box (Z direction) ensured that all the solvent molecules remain inside the simulation box throughout the simulations. This "two charged surface assembly" also facilitated the motion of the peptide inside the simulation box toward the oppositely charged surface, which otherwise would not have taken place. The computational cost of the simulations was also reduced considerably as compared to a "single surface assembly".

Canonical MC simulations were carried out at 298 K. The rectangular simulation box consisted of a single peptide molecule, the surface, and a fixed number of solvent molecules. The solvent density was calculated from the mole fractions of each component in the solvent mixture. The volume used in calculating the solvent density was equal to the volume of the box minus the volume occupied by the peptide. The number of solvent molecules was adjusted in each case so as to get the desired mole fraction and density for the solvent mixture inside the simulation box. The dimensions of the box for each cosolvent system were kept constant whereas the number of solvent molecules was changed to obtain the desired density. For example, for the methanol−water system, the dimensions of the box were 27.748 Å × 24.030 Å × 38.00 Å, and for the glycerol−water system, the dimensions of the box used were 31.355 Å × 27.154 Å × 36.00 Å. The density of each solvent mixture and the number of solvent molecules are reported in Tables 5 and 6.

All of the interactions in this work were calculated using the minimum image (MI) convention.[23] Song and Forciniti[24] found out that there was a negligible difference between pair correlation functions generated using Ewald summation[25] and those obtained using the MI convention. They showed that the use of the MI convention was sufficient to generate qualitatively reliable properties, like PCFs and density profiles, which do not depend strongly on the treatment of long-range interactions.[26]

The 8-residue peptide was simulated in bulk solvent (in the absence of the walls) to study the effect of changes in solvent composition on its conformation in the nonadsorbed state. A representative sample of the ensemble of true nonadsorbed states was thus obtained, which was used as the starting conformation of the peptide in all of the simulations in the presence of the surface. The peptide was initially kept at the center of the box and then allowed to move. The magnitudes of the maximum translational and rotational movements for the solvent molecules were set separately. The peptide was given a translational and rotational movement followed by torsional movement. Each torsional movement[15] consisted of changing the Φ (torsion angle formed by four atoms C−N−C$_\alpha$−C) and the Ψ (torsion angle formed by four atoms N−C$_\alpha$-C−N) angles of all the residues; this combination of moves yields the lower energy configuration of the system.

Pair correlation functions (PCFs) were calculated between selected peptide atoms and solvent molecules. The PCFs were calculated by counting the number of solvent atoms in spherical shells at different distances (r) from a peptide atom and dividing these numbers by the product of solvent density and shell volume. When the peptide goes to the surface, a portion of the volume around the peptide is inaccessible to the solvent because it is occupied by the surface. Therefore, the presence of the surface affects the PCFs to some extent depending upon the distance between the peptide atom and the surface. We accounted for this by excluding the volume occupied by the surface in the calculation of PCFs.

The amount of solvent next to any atom of the peptide can be estimated by calculating the coordination number between any atom in the peptide and the solvent. The coordination number (N) around any peptide atom, α, is defined as

$$N_{\alpha S} = 4\pi\rho_S \int_0^{r_c} r^2 g_{\alpha S}(r)\, dr \qquad (4)$$

where S is the selected atom of the solvent (oxygen of water and methanol, CH of glycerol), ρ_S is the solvent number density, and $g_{\alpha S}(r)$ is the PCF between atom α and S. The upper limit of integration in eq 4 is not a well-defined quantity because of difficulties in defining "solvation" layer. A reasonable choice for the upper limit of integration is the van der Waals diameter of water (3.329 Å); that approached was followed here to calculate peptide−water coordination numbers. Coordination

Table 3. (a) Effective LJ Parameters for the Glycerol Model[22] and (b) Effective Charge and Geometrical Parameters for the Glycerol Model[22]

(a)

A_{OO} (Å-K$^{1/12}$)	C_{OO} (Å-K$^{1/6}$)	$A_{CH_1CH_1}$ (Å-K$^{1/12}$)	$C_{CH_1CH_1}$ (Å-K$^{1/6}$)	$A_{CH_2CH_2}$ (Å-K$^{1/12}$)	$C_{CH_2CH_2}$ (Å-K$^{1/6}$)
4.877	8.049	5.772	8.768	6.179	9.741

(b)

q_O (e)	q_{CH_2} (e)	q_{CH_1} (e)	q_H (e)	L_{OCH_2/CH_1} (Å)	$L_{CH_2CH_1}$ (Å)	L_{OH} (Å)	θ_{CCC} (°)	θ_{CCO} (°)	θ_{HOCH_1} (°)
−0.34	0.0	0.0	+0.34	1.410	1.509	0.955	109.5	109.5	108.5

A_{OH}, A_{HCH_2}, and A_{HCH_1} are equal to zero.

Table 4. Effective Pair Potential Parameters and Partial Charge for Peptide Atoms and Surface Atoms

atom γ	$A_{\gamma\gamma}$ (Å-K$^{1/12}$)	$C_{\gamma\gamma}$ (Å-K$^{1/6}$)	q_γ (e)
	Peptide		
C	5.216	8.096	0.38
CA, CB_2	6.730	10.703	0
CB_1, CG_1	6.344	10.152	0
CD, CG_2	6.187	10.110	0
CG	5.216	8.096	0.27
H	0.000	0.000	0.28
N	4.925	8.150	−0.28
O	4.598	8.050	−0.38
OD_1, OD_2	4.598	8.050	−0.635
	Surface		
CH_2[a]	6.344	10.152	±0.0800[b] ±0.1021[c]

[a] $\sigma_{CH_2} = 3.964$ Å; $\epsilon_{CH_2} = 70.49$ K. [b] Charged surfaces (charge on each site for methanol−water simulation). [c] Charged surfaces (charge on each site for glycerol−water simulation).

numbers are reported for selected atoms of the peptide, i.e., O and N of peptide bond and OD_1 and OD_2 side chain atoms of the aspartic acid residue.

Solvent density profiles and pair correlation functions between surface sites and solvent molecules were generated to study the displacement of solvent molecules close to the surface by the peptide (dehydration of the surface). The solvent density profile was generated by dividing the simulation box into small slabs (0.05 Å) in the Z direction, and the profiles were calculated by counting the number of constituent atoms of the solvent in each slab. To generate PCFs between surface sites and solvent molecules, we constructed a semispherical shell of radius r with the surface site X at the center, counted the number of constituent atoms of solvent molecules in each shell, and divided that number by the product of solvent density and the semi-shell volume.

Ramachandran Plot.[27] The extent of the reorganization of the peptide at the surface was determined by monitoring the torsion angle (ϕ,Ψ) map, which is known as the Ramachandran plot. Ramachandran plots were constructed using the torsion angles of the peptide generated during the production run of the simulation. In addition to mapping the conformational space sampled by the peptide at the surface, these plots were used to corroborate the RasMol definitions of structures (such as helix, turn and random coil).

Peptide End-to-End Distance.[28] The 8-residue peptide's end-to-end distance was defined as the distance separating the N atom of the N-terminal ASP[1] residue and the C^α of the C-terminus ILE.[8] That calculation is equivalent to the definition

$$r_l = \sum_i \upsilon_i \tag{5}$$

where υ_i is the vector connecting the consecutive N atoms along the backbone between the N- and C-termini. The ensemble average $\langle r_l^2 \rangle$ was computed by averaging over all the Monte Carlo steps. Changes in the values of r_l are a good indication of a significant reorganization of the peptide's global structure. The ensemble average end-to-end distance of the peptide was compared to its original helix length.

RasMol.[29] RasMol was used in this work to obtain a snapshot of the simulation box at the end of the simulation. Based on the torsion angles and intrinsic hydrogen bonding network of the peptide, RasMol was used to identify the peptide's secondary structure at the surface. The secondary structures observed in

Table 5. Water−Methanol Systems: Density and Number of Molecules

system	number of water molecules	number of methanol molecules	density (g/cm^3) simulations	density (g/cm^3) experimental
100% water	820	0	1.0000	1.0000
75% water + 5% methanol	486	162	0.9466	0.9567
50% water + 50% methanol	264	264	0.8933	0.9088
30% water + 70% methanol	136	316	0.8506	0.8644
100% methanol	0	376	0.7866	0.8460

Table 6. Glycerol−Water Systems: Density and Number of Molecules

system	number of water molecules	number of glycerol molecules	density (g/cm^3) simulations	density (g/cm^3) experimental
100% water	998	0	1.000	1.000
93% water + 7% glycerol	734	55	1.0183	
85% water + 15% glycerol	545	96	1.0392	
70% water + 30% glycerol	337	144	1.0783	

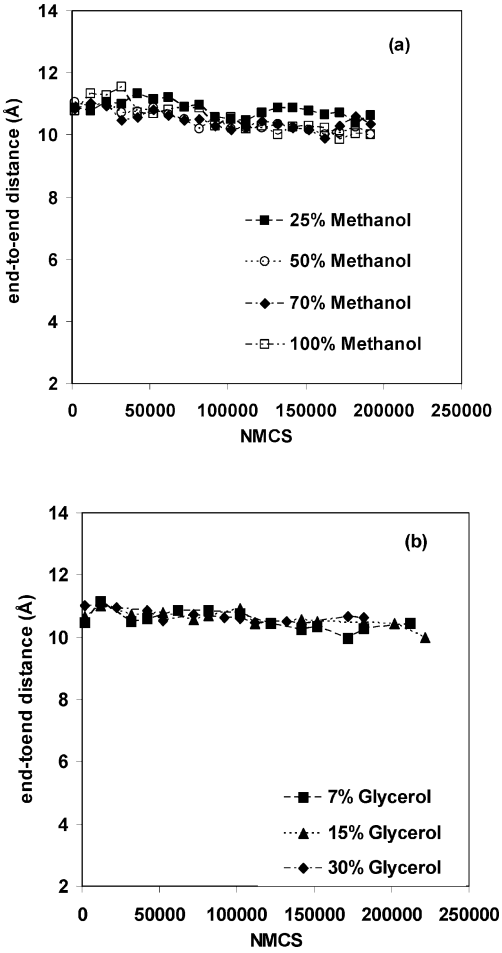

Figure 1. End-to-end distance (Å) vs the number of Monte Carlo steps (NMCS) for the peptide in bulk (nonadsorbed) at various solvent compositions. (a) Three different methanol−water mixtures and pure methanol. (b) Three glycerol−water mixtures.

our simulation were helices, turns and random coils. Residue '*i*' is involved in helix formation if the torsion angles fall within a specified range; that is, $\phi(i)$ is −57.0° and Ψ(i) is −47.0°. An inverse gamma turn is defined for 3 residues (i, $i+1$, $i+2$) if a hydrogen bond exists between first (i) residue and last ($i+2$) residue and the ϕ and Ψ angles of residues $i+1$ fall within a specified range: $\phi(i+1)$ is −79.0° and $\Psi(i+1)$ is 69.0°.[30,31] Random coils are formed by the segments of the peptide chain that do not organize themselves in a regular secondary structure. RasMol represents helices by "red", turns by "pale blue", and random coils by "white". The structure of the peptide was determined by using these definitions and the results were compared with the information obtained from Ramachandran plots.

The simulation programs were written in FORTRAN90 and can be executed on different machines. All of the simulations were performed on a Dual Xeon Pentium-IV processor running at 2 GHZ. Programs were compiled using Intel FORTRAN Compiler 8.1 for Linux. The amount of CPU time required for 420 000 steps depended on solvent composition because of the different number of solvent molecules needed in each case. For example, with 820 water molecules (0% methanol system), the system took approximately 160 h for the 8-residue peptide in the presence of the surface to complete 420 000 steps.

Results and Discussion

MC simulations of the peptide in bulk solvents were performed to study its conformational stability in the nonadsorbed state. End-to-end distances and Ramachandran plots were used to monitor changes in peptide conformation. Figure 1, panels a and b, shows the change in end-to-end distance of the peptide with the number of Monte Carlo steps (NMCS) at different solvent compositions. Despite some degree of rearrangement, the original helical structure of the peptide was maintained. This is confirmed by the Ramachandran plots shown in Figure 2, panels a and b. The Φ and Ψ torsional angles did not deviate from the original helix angles but fraying at two ends (i.e., ILE[8] residue) was observed for all cases. Therefore, it can be concluded that the peptide shows minimal or no structural instability in any solvent composition, which facilitates the analysis of the behavior of the peptide at solid/liquid interfaces. The stability of the peptide at high concentrations of methanol is, somehow, puzzling. We have observed that the

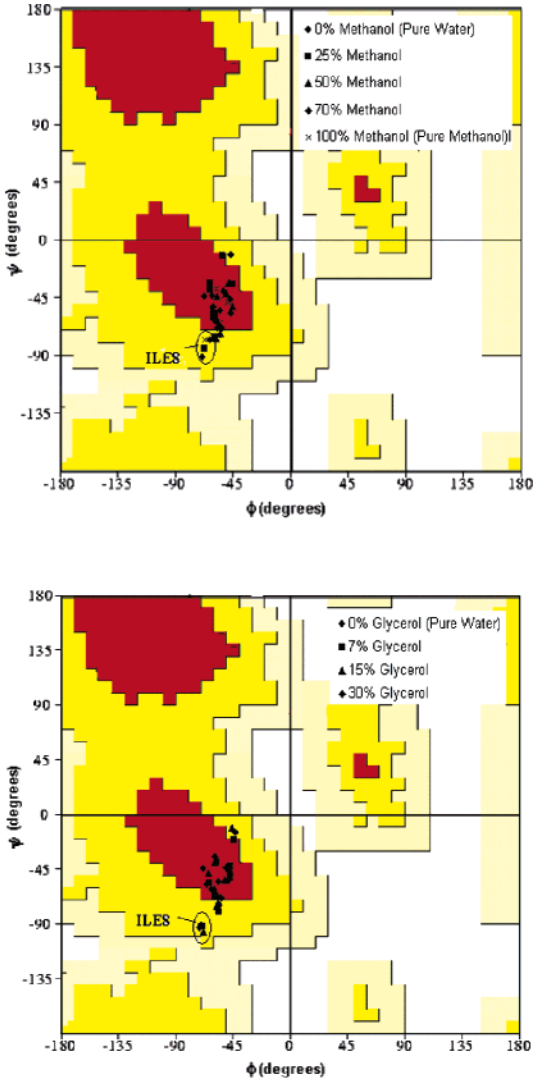

Figure 2. Ramachandran plot of the peptide in bulk (nonadsorbed state) at various solvent compositions. (a) Pure water, three different methanol−water mixtures and pure methanol. (b) Pure water and three different glycerol−water mixtures.

Table 7. Initial Conditions Used in the Simulations[a]

MC run	θ	Z	MC run	θ	Z
1	40	0	3	0	3.6
2	80	0	4	0	6.0

[a] θ = angle of rotation (degrees) of the end-to-end (N−C) vector of the peptide with respect to z unit vector (which is normal to the surface). Z = distance (Å) of the peptide from the center of the simulation box toward the positively charged surface.

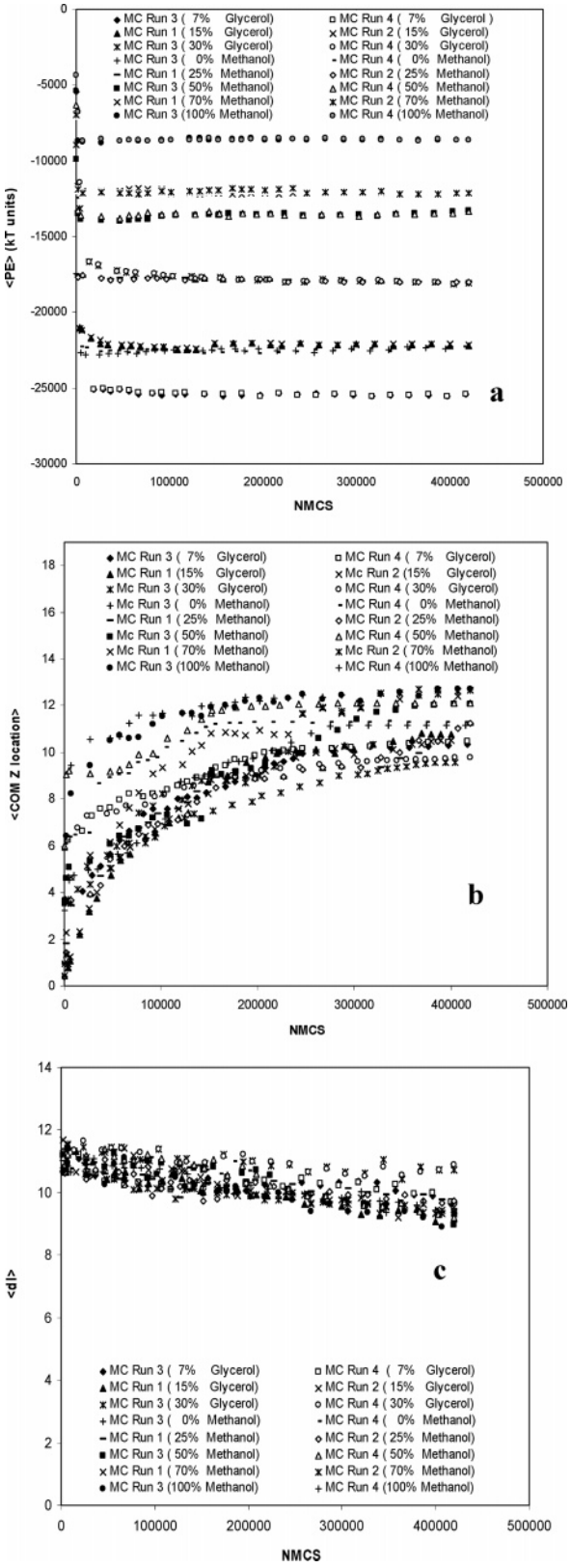

Figure 3. Statistical conversion test with different orientations and distances of the peptide (Identified by different MC Run numbers, Refer to Table 7 for details) with respect to the surface at various solvent compositions such as pure water, three different methanol−water mixtures, pure methanol and three different glycerol-water mixtures. (a) potential energy (PE) vs number of Monte Carlo steps (NMCS). (b) *Z* location of the center-of-mass (COM) (Å) of the peptide from the surface vs number of Monte Carlo steps (NMCS). (c) End-to-end distance (⟨*d*⟩, Å) of the peptide vs number of Monte Carlo steps (NMCS).

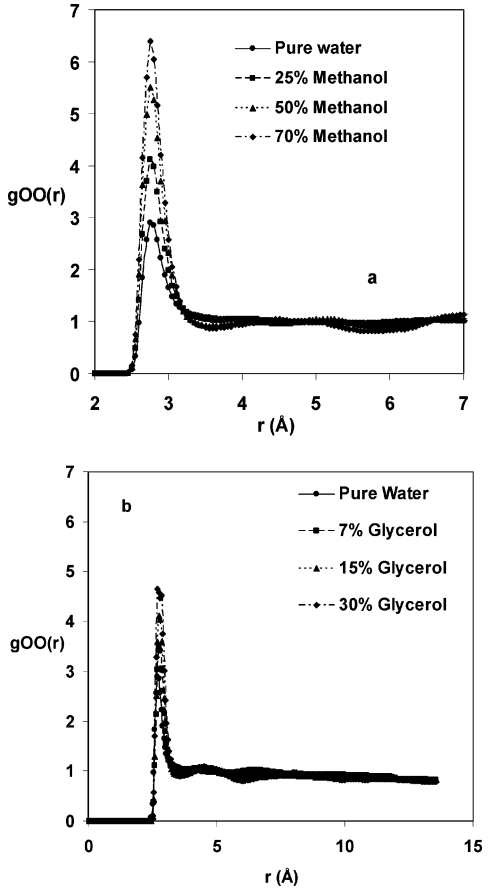

Figure 4. Radial distribution functions for oxygen of water at various solvent compositions. (a) Pure water and three different methanol−water mixtures. (b) Pure water and three different glycerol−water mixtures.

conformation of much longer homo peptides (more than 20 residues) is sensitive to solvent composition; so, we speculate that both the sequence of the eight residue peptide and its very short length stabilize the helix. It may be also possible that the peptide is trapped in its helical conformation and other conformations of slightly lower energy are not accessible. Either way, it is expected that differences in the adsorption behavior at different solvent compositions do not arise from differences in its bulk conformation because the peptide native structure is not disrupted in the nonabsorbed state.

The center-of-mass (COM) of the peptide was placed equidistant from the positively and negatively charged surfaces, i.e, at the center of the box. We defined an orientation vector that connects the α-carbon atoms of the first and last residues. The order parameter, s_0^2, and the *Z* location profiles of selected peptide atoms were monitored to determine the orientation and position of the peptide after equilibration. The order parameter is defined as

$$S_0^{\,2} = \langle 3\cos^2\theta - 1\rangle/2 \qquad (6)$$

where θ is the angle between the peptide orientation vector and the normal to the surface. If S_0^2 equals 1, the peptide orientation vector is perpendicular to the surface. If its value is −0.5, the orientation vector is parallel to the surface. If it is zero, the peptide is randomly oriented throughout the simulations. *Z* location profiles were calculated for three sites: the N atom of the first ASP residue, the CD atom of the last ILE residue, and the COM of the peptide. It is important to notice that the orientation vector may change during the course of the simula-

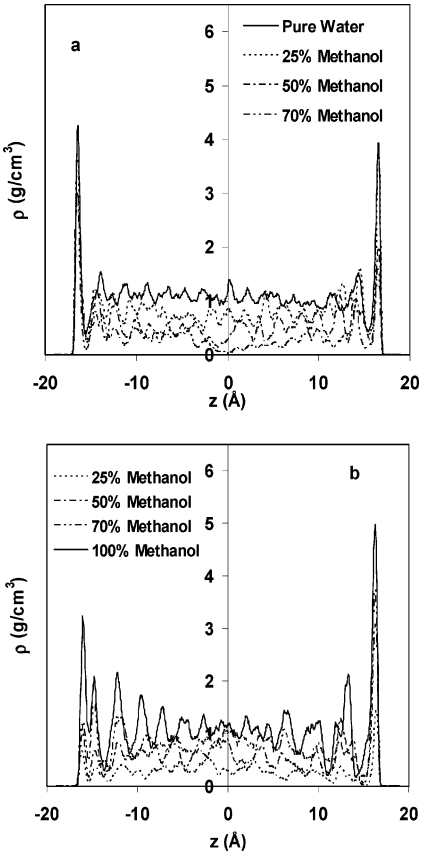

Figure 5. Solvent density (ρ in g/cm^3) profiles between charged surfaces at various methanol−water solvent compositions. The right side is the positively charged surface (located at 19 Å) and the left side is the negatively charged surface (located at −19 Å). (a) Density profile of oxygen of water for pure water, three different methanol−water mixtures. (b) Density profile of oxygen of methanol for three different methanol−water mixtures and pure methanol.

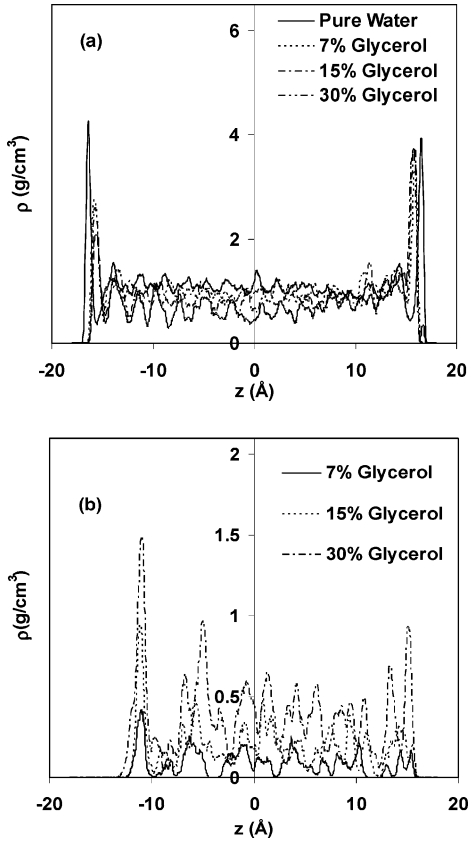

Figure 6. Solvent density (ρ, g/cm^3) profiles between charged surfaces at various glycerol-water solvent compositions. The right side is the positively charged surface (located at 18 Å), and the left side is the negatively charged surface (located at −18 Å). (a) Density profile for oxygen of water for pure water and three different glycerol−water mixtures. (b) Density profile for oxygen of glycerol for three different glycerol−water mixtures.

tion if there are changes in the conformation of the peptide. Therefore, visualization of the peptide helps eliminating misinterpretation of the data. Z location profiles were generated by collecting the Z coordinates of the sites over the production run and calculating the probability of locating them at different distances from the surfaces.

Multiple simulations of the peptide at the surface in the chosen solvent compositions were performed to explore the possibility of including biases by placing the peptide in a particular location and orientation at the start of the simulation. Four simulations starting with different initial orientations and locations of the peptide with respect to the surface were performed (Table 7 summarizes the conditions used for these runs). Each simulation consisted of 2.8×10^5 equilibration steps and 1.4×10^5 production steps. All of the movements were adjusted every 25 steps to maintain an acceptance ratio of 50% throughout the simulation. One MC step consists of $N_{solvent} + N_{cosolvent} + 1$ movements (moving each solvent and cosolvent molecule and the peptide molecule in the simulation box once). All simulations gave qualitatively and quantitatively consistent results. Representative Monte Carlo runs showing the potential energy of the system, location of the center of mass (COM) of the peptide, and end-to-end distance of the peptide as a function of NMCS are shown in Figure 3a−c. The potential energy (PE) at different solvent compositions as a function of NMCS is shown in Figure 3a. After the first ∼25 000 steps, all runs converge to the same potential energy value for each solvent composition. The location of the COM of the peptide as it moves from the center of the box toward the positively charged surface as a function of NMCS is shown in Figure 3b. The COM in all cases maintains nearly the same location for each solvent composition. The end-to-end distance of the peptide is spread around a value of ∼10.25 Å (Figure 3c). This spreading in the end-to-end distance confirms that in all the simulations the peptide's conformation changes, which is discussed in detail in following paragraphs. The peptide was placed with its orientation vector perpendicular to the surface at the center of the box for the remaining runs. The peptide moves toward the surface of complementary electrostatic charge.

Methanol−water and glycerol−water mixtures have been extensively studied by various authors.[32,33] Methanol and glycerol affect the properties of pure water because of their different hydrogen bonding capability, hydrophobicity, and dielectric properties. Hydrogen bonding capacity increases in the following order: glycerol ≫ water > methanol. Water is a double H-bond donor, and methanol is a single H-bond donor, whereas both of them are double H-bond acceptors. Glycerol, because of its three hydroxyl groups, has the highest hydrogen bonding capacity. The dielectric constants of methanol−water and glycerol−water mixture are below that of water, and they vary linearly with composition.[33,34] Finally, methanol is considered to be more hydrophobic than water, whereas glycerol is more hydrophilic. Thus, it is expected that both alcohols would then change hydrogen bonding capacity, enhance the electrostatics interactions, and exert opposite effects on the hydrophobic interactions. These changes in the properties of methanol−water and glycerol−water mixtures, the heterogeneity of the adsorbate, and the properties of adsorbent surface generate a complex set of in-

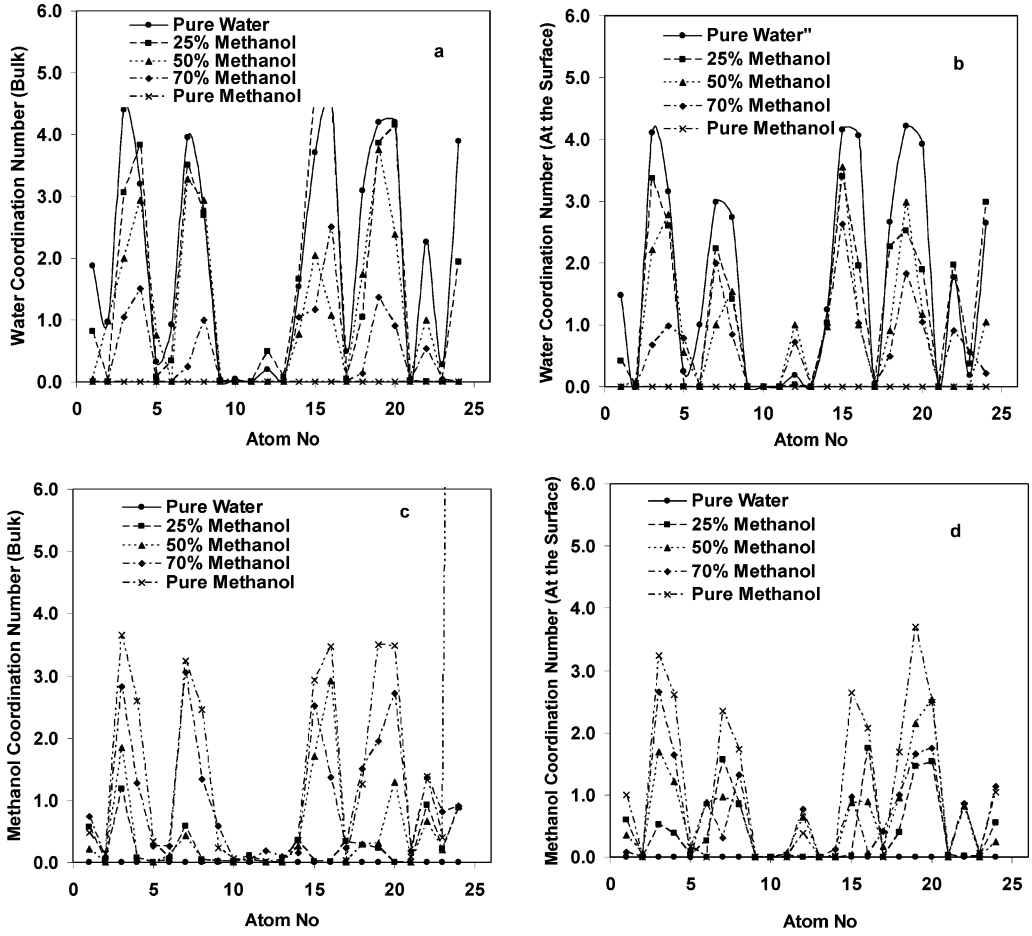

Figure 7. Solvent-peptide coordination numbers at various methanol−water solvent compositions in the bulk (nonadsorbed state) and at the surface (adsorbed state) for selected peptide atoms. (a) Water−peptide coordination numbers for pure water, three different methanol−water mixtures and pure methanol in bulk. (b) Water−peptide coordination numbers for pure water, three different methanol−water mixtures and pure methanol at the surface. (c) Methanol−peptide coordination numbers for three different methanol−water mixtures and pure methanol in bulk. (d) Methanol-peptide coordination numbers for three different methanol−water mixtures and pure methanol at the surface.

terrelated interactions. To isolate the effect of solvent on adsorption, solvent−solvent, solvent−surface, and solvent−peptide interactions were studied independently and then correlated with the observed behavior of the peptide at the surface.

Changes in solvent−solvent interactions because of addition of alcohols were examined in this work by monitoring radial distribution functions (RDFs) of selected atoms of water and methanol or glycerol. For example, changes in water−water interactions because of the addition of alcohols were studied by observing RDFs of oxygen of water (Figure 4, panels a and b). The magnitude of the first maximum of $g_{OO}(r)$ between oxygen atoms of water (Figure 4, panels a and b) increases with increasing methanol and glycerol concentrations. The RDFs also suggest that oxygen−oxygen nearest distances are independent of methanol or glycerol concentration. This behavior of the RDFs confirms the observation that water is more structured in the presence of methanol and glycerol.[34,35] Comparison of the RDFs suggests that methanol is a stronger water-structure maker than glycerol (i.e, a higher degree of association between water molecules is observed in the presence of methanol). Moreover, the structure between water−alcohol and alcohol−alcohol is also enhanced. On the basis of the peak areas of the corresponding RDFs, we conclude that "the strength" in the association of solvent molecules (in solvent mixtures) follows the trend: water−water ≫ water−alcohol > alcohol−alcohol. Thus, the number of water or alcohol molecules "available" to associate with the peptide or the surface would decrease when both solvents are in the presence of each other because of a stronger solvent−solvent association. For example, for the methanol−water system, the stronger water−water interactions, observed as the methanol concentration is increased, leads to a decrease in the availability of water molecules that can interact with the peptide and the surface. This would result in a stronger interaction of the peptide with the surface. The effect of these changes in solvent−solvent association on solvent-surface and solvent−peptide interactions will be discussed in the subsequent sections.

Solvent−surface interactions or rearrangement of solvent molecules at the surface play an important role in the behavior of the peptide at the surface.[15] Solvent−surface interactions are expected to change because of changes in solvent composition. Solvent density profiles were used in this work to qualitatively study those changes. Solvent density profiles at different concentrations of methanol are plotted in Figure 5, panels a and b. Figure 5a shows a decrease in the density of water molecules at the surface with increasing methanol concentration, whereas the opposite effect was observed for the concentration of methanol at the surface (Figure 5b). Therefore, the positively charged surface is preferentially solvated by methanol at higher concentrations of the alcohol. As discussed previously, a stronger water−water association is mainly responsible for this behavior. We can speculate at this point that the peptide would replace methanol from the surface easier than water because water is more polar than methanol. This would induce a stronger interaction between the peptide and the surface in the presence of alcohol. Figure 6, panels a and b, shows the density profiles

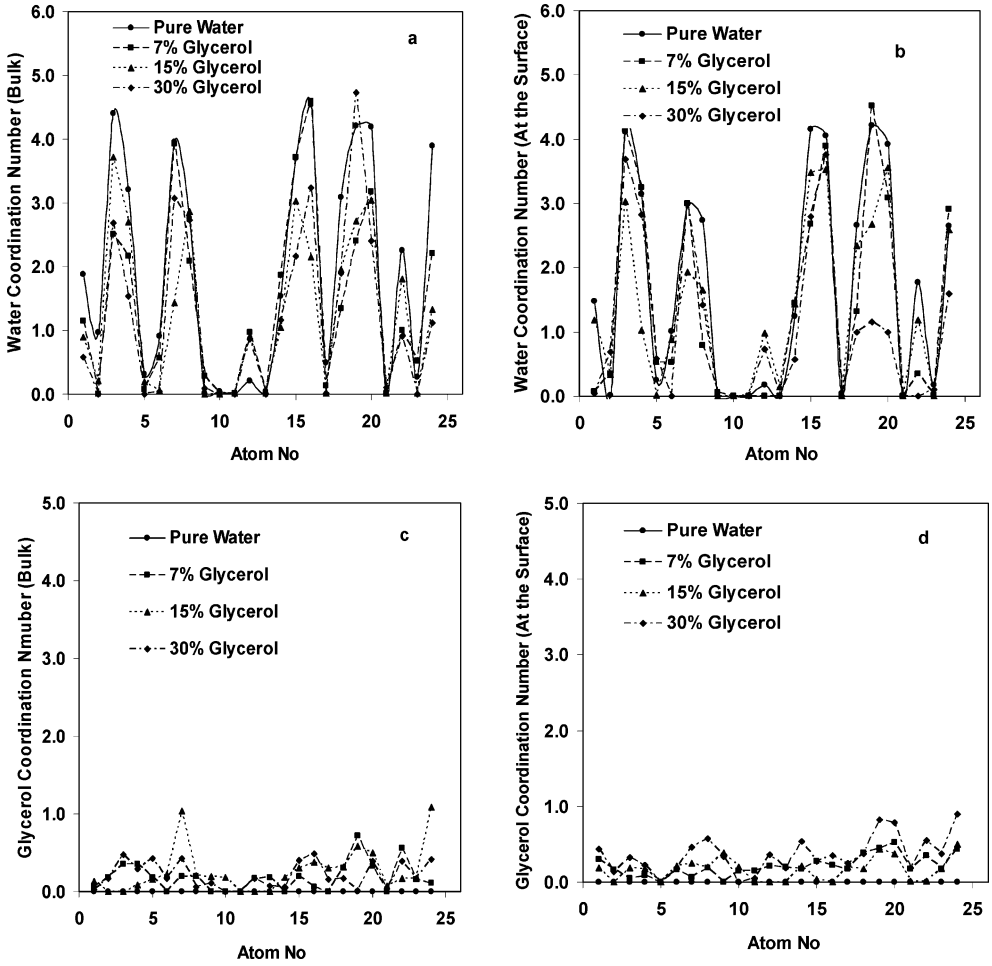

Figure 8. Solvent−peptide coordination numbers at various glycerol−water solvent compositions in the bulk (nonadsorbed state) and at the surface (adsorbed state) for selected peptide atoms. (a) Water−peptide coordination numbers for pure water and three different glycerol-water mixtures in bulk. (b) Water−peptide coordination numbers for pure water and three different glycerol−water mixtures at the surface. (c) Glycerol−peptide coordination numbers for three different glycerol−water mixtures in bulk. (d) Glycerol−peptide coordination numbers for three different glycerol−water mixtures at the surface.

of water oxygen and of the oxygen of glycerol between the two solid surfaces with increasing glycerol concentration. We believe that strong glycerol−glycerol interactions and steric effects are responsible for the depletion of glycerol at the surface. In this case, the surface remains solvated mainly by water; this is evident in Figure 6a that shows very little or no change in the density of water between the surfaces as a result of the addition of glycerol. Thus, our results suggest a weakening of the water−surface interaction as a result of the addition of methanol but no change in the strength of water−surface interactions as a result of the addition of glycerol.

As reported in our earlier work,[15] water−peptide interactions do play an important role in determining the behavior of peptides at solid surfaces. Water−peptide interactions are expected to change considerably because of the addition of cosolvents. As discussed above, methanol and other monohydric alcohols decrease the magnitude of the hydrophobic interaction as a result of increased interaction of methanol with the nonpolar residues of the peptide. On the contrary, glycerol is expected to increase the magnitude of hydrophobic interactions because glycerol will be preferentially excluded from the nonpolar residues of the peptide.[36] Although both pair correlation functions and solvent coordination numbers of selected peptide atoms can be used to quantify the interaction between the solvent and the peptide, the following discussion is limited to coordination numbers of selected peptide atoms because they offer a clearer picture than pair correlation functions. Panels a and b in Figure 7 show water

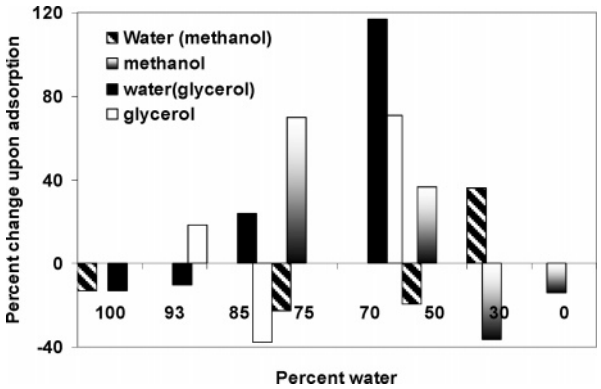

Figure 9. Percent change (amount of solvent bound after adsorption amount of solvent bound in bulk) versus percent water in the solvent. Water(methanol) refers to water in water methanol mixtures and water(glycerol) refers to water in water glycerol mixtures.

coordination numbers for selected peptide atoms in bulk (nonadsorbed state) and at the surface (adsorbed state), respectively, whereas panels c and d in Figure 7 show methanol coordination numbers for selected peptide atoms in bulk (nonadsorbed state) and at the surface (adsorbed state), respectively. In all cases (i.e., adsorbed and nonadsorbed states of the peptides), the charged side chain atoms (OD_1 and OD_2) of all of the aspartic acid residues (atom numbers 3, 4, 7, 8, 15, 16, 19, and 20) remained moderately or highly solvated with water

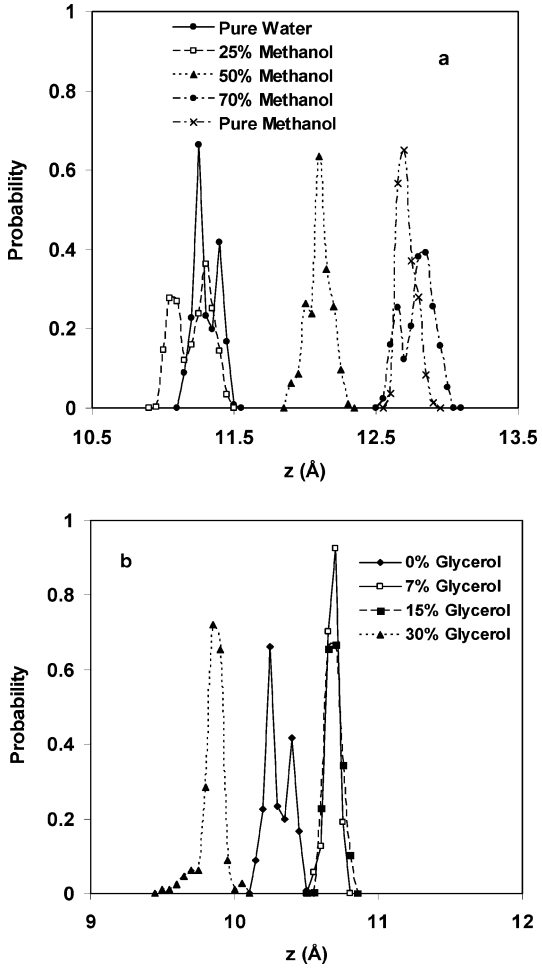

Figure 10. *Z* location (Å) of center-of-mass (COM) of the peptide at various solvent compositions. (a) Pure water, three different methanol−water mixtures and pure methanol. (b) Three different glycerol−water mixtures.

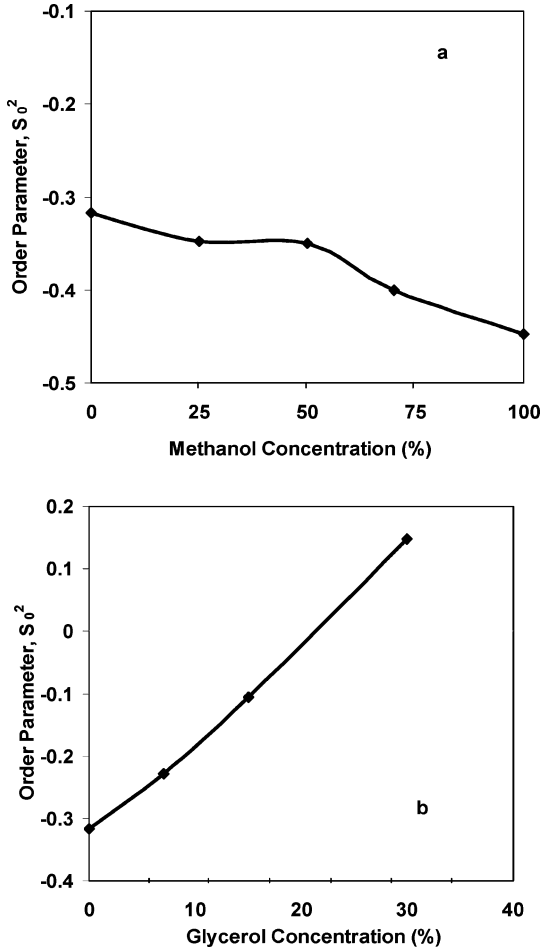

Figure 11. Order parameter of the peptide molecule vs methanol or glycerol concentration. (a) Pure water, three different methanol−water mixtures and pure methanol. (b) Pure water and three different glycerol−water mixtures.

and methanol (with coordination numbers ranging from 1 to ∼5). The peptide bond atoms O and N of ASP[1], ASP[2], ASP[5], and ASP[6] (atom numbers 1, 2, 5, 6, 13, 14, 17, and 18) and ILE[3] and ILE[4] (atom numbers 9, 10, 11, and 12) remained solvent depleted (with coordination numbers less than 1). Peptide bond atoms of the end-terminal isoleucine residues, ILE[7] and ILE[8] (atom numbers 21, 22, 23, and 24), remained moderately or highly solvated (with coordination numbers ranging from 1 to 4) in all cases. At a high methanol concentration, the peptide is solvated mainly by methanol rather than water both in bulk and in the adsorbed state. Very few free water molecules are available for interaction with peptide atoms at high methanol concentrations; therefore, the peptide becomes solvated by the alcohol. A similar analysis of coordination numbers in the presence of glycerol is shown in Figure 8a−d. Glycerol remains excluded from the peptide in both the adsorbed and the nonadsorbed states, which is evident from coordination numbers lesser than 1. Because peptide−water coordination numbers in the presence of glycerol are similar to those observed in pure water and because methanol seems to induce the dehydration of the peptide (compare Figure 7, panels a and b, with Figure 8, panels a and b), one can conclude that water is more tightly bound to the peptide atoms in the presence of glycerol. Despite the similarities between the hydration patterns in the presence of various solvents, there are some significant differences in the overall hydration. Figure 9 shows the percent change in hydration of the peptide upon adsorption in the presence or absence of the cosolvents. There is approximately a 15% decrease in hydration when the peptide adsorbs from pure water. Above 50% methanol the polar groups in the peptide are preferentially hydrated and methanol is excluded from their vicinity. Except at very low concentrations of glycerol (less than 7%), the presence of glycerol drastically increase the amount of water "bound" to the peptide. Overall, at 30% glycerol there is an increase of both glycerol and water in the vicinity of the peptide at the surface.

The simulations show that the equilibrium position of the COM of the peptide at the surface is a function of methanol and glycerol concentrations (Figure 10, panels a and b). This dependence with cosolvent concentration reflects the effect of the changes in solvent−solvent, solvent-peptide and solvent-surface interactions discussed above. The COM of the peptide is located at a distance from the positively charged surface (the surface is located at 19 Å in the Figure 10a) of ∼7.75 Å for 0% and 25% methanol, at a distance of 6.9 Å for 50% methanol, and at a distance of ∼6.3 Å for 70% and 100% methanol. Therefore, the COM shifts toward the surface as the concentration of methanol is increased. The COM of the peptide is located at a distance of ∼7.3 Å for 7% and 15% glycerol and 8.15 Å for 30% glycerol from the positively charged surface (the surface is located at 18 Å in the Figure 10b). Broadening of the peaks observed in methanol−water mixtures can be attributed to weak solvent-peptide interactions that increase the flexibility of the peptide as compared to glycerol−water system. Even though the flexibility increases, direct contact of the charged peptide

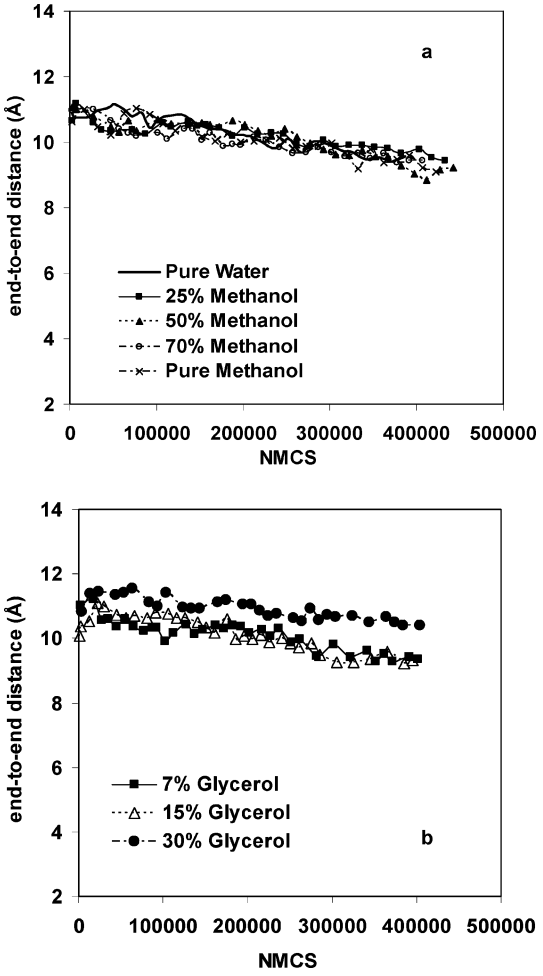

Figure 12. End-to-end distance (Å) vs number of Monte Carlo steps (NMCS) of the peptide at the surface at various solvent compositions. (a) Pure water, three different methanol−water mixtures and pure methanol. (b) Three different glycerol−water mixtures.

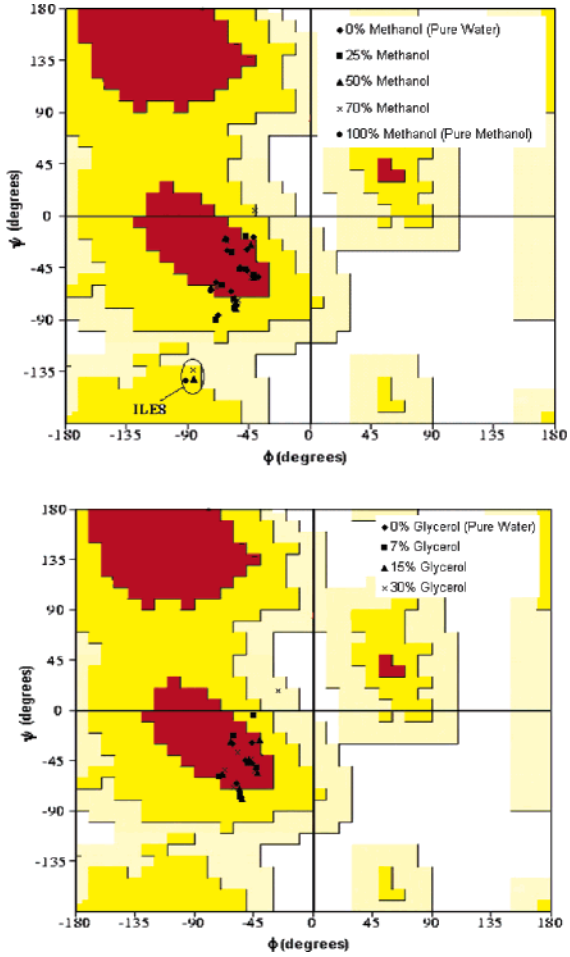

Figure 13. Ramachandran plot for the peptide at the surface at various solvent compositions. (a) Pure water, three different methanol−water mixtures and pure methanol. (b) Pure water and three different glycerol−water mixtures.

atoms with the surface did not occur because of the low surface charge density. Therefore, the gross conformation of the peptide is maintained upon adsorption; this is discussed in following sections.

The orientation of the peptide at the solid/liquid interface changes as the solvent composition is changed. Figure 11a clearly shows that the peptide orients more parallel to the surface as the methanol concentration is increased. On the contrary, the peptide aligns perpendicular to the surface as the glycerol concentration is increased (Figure 11b). It is, of course, impossible to quantify the amount adsorbed because the simulations were done at infinite dilution. However, one can infer a correlation between the orientation of the peptide and the amount adsorbed. It is obvious that the amount adsorbed will be larger if the peptide adsorbs end-on because a side-on orientation would occupy a much larger surface. Therefore, the amount of peptide adsorbed would be reduced in the presence of methanol while it would be increased in the presence of glycerol, which qualitatively agrees with experimental reports.[11−12]

In our previous adsorption studies,[15] using the same peptide dissolved in pure water, we observed that the peptide undergoes minimal or no change in conformation in the adsorbed state. We attributed this behavior mainly to the strong hydrogen bonding network of the peptide and strong water−surface interactions (we observed a solvent layer trapped between the surface and the peptide). A similar observation is being made in the current study. An analysis presented earlier for solvent-peptide interactions based on solvent coordination numbers of selected peptide atoms, showed that the peptide bond atoms (O and N) in the adsorbed state remained depleted of solvent. As a result of that, the original backbone hydrogen bonding network and thus most of the helical structure is maintained at all solvent compositions in the adsorbed state. The surface charge density (0.02711e/Å^2) used in this work was lower than the charge density of 0.09055e/Å^2 used in our earlier work.[15] Therefore, with the current charged density, peptide−surface interactions are not strong enough to replace the solvent (especially water at low methanol and all glycerol concentrations) layer at the surface. The result of this is that direct contact of the peptide charged side chain atoms (OD1 and OD2) with the surface is not possible at low methanol concentration (0% and 25%). A similar conclusion can be reached at all glycerol concentrations. As the methanol concentration was increased up to 50% or higher, the charged peptide atoms interact strongly with the surface and thus some degree of rearrangement of the peptide is observed, this is evident from the end-to-end distance (Figure 12, panels a and b) and Ramachandran plots (Figure 13, panels a and b) of the peptide in the adsorbed state at these methanol concentrations. The Ramachandran plot shows that, although the Φ and Ψ torsional angles of most residues remain inside the helical region, the end-terminal ILE[8] forms a fraying end in the adsorbed state. The strength of solvent−surface interaction weakens in the presence of higher methanol concentration because the surface is solvated mainly by methanol at higher concentrations of the alcohol. Thus, the charged peptide atoms

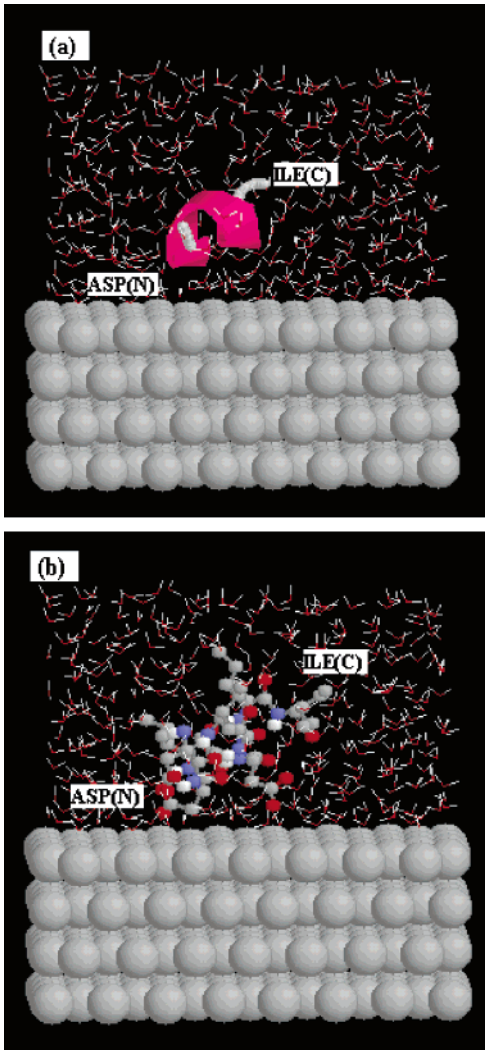

Figure 14. Visualization of the peptide at the surface in 100% water (a) cartoons view of the peptide (b) ball-and-stick view of the peptide. Methyl groups are gray; nitrogen atoms are blue; oxygen atoms are red; hydrogen atoms are white. Water molecules are represented by wireframes, where oxygen atoms are red and hydrogen atoms are white.

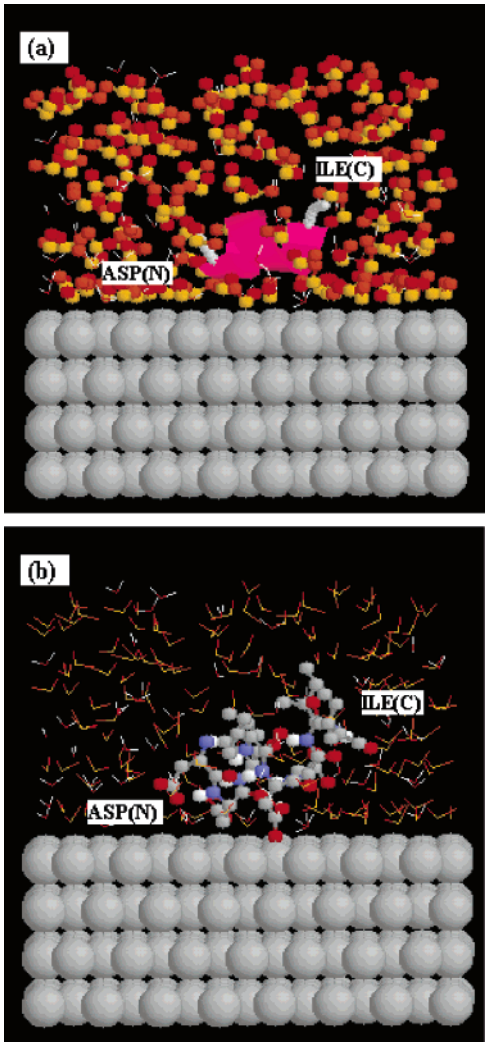

Figure 15. Visualization of the peptide at the surface in 70% methanol (a) cartoons view of the peptide; ball-stick-view of methanol; wireframes view of water (b) ball-and-stick view of the peptide; wireframes view of water and methanol. Methanol oxygen atoms are yellow; methanol methyl groups are orange; methanol hydrogen atoms are red. Water and peptide color code remains the same as in Figure 14.

can closely approach the surface by replacing some of the methanol molecules at the surface. These features (particularly the orientation and conformational changes upon a solvent change) can be visualized by using RASMOL. Three systems, 100% water (or 0% methanol), 70% methanol and 30% glycerol, are shown in Figures 14−16, respectively. These pictures confirm the observed changes in orientation and conformation upon addition of the cosolvents. For example, Figure 14b shows that the OD_1 and OD_2 atoms of the ASP^2 residue are closer to the surface in 70% methanol than in either 100% water or 30% glycerol. The consequence of this close interaction with the surface is the structural rearrangement of the peptide that is observed in the cartoon. As discussed previously, despite these structural rearrangements the peptide maintains its helical structure as can be seen in Figures 14a, 15a, and 16a, which show a single helical segment (in pink color) for the adsorbed peptide. Figures 14a, 15a, and 16a also confirm the different orientations of the peptide in the adsorbed state induced by changes in solvent composition. For example, Figure 15a clearly shows that the peptide axis is parallel to the surface in 70% methanol, whereas it is inclined at an angle in 100% water and 30% glycerol. Furthermore, RASMOL visualization helps to understand and confirm the observed distribution of solvent molecules at the surface at different solvent compositions. For example, Figure 15 shows that the surface is solvated mainly by methanol molecules at 70% methanol concentration, while Figure 16 confirms that the surface remains solvated by water molecules at 30% glycerol.

Conclusions

Monte Carlo simulations were used to study the effect of solvent composition on the adsorption of a short peptide at a liquid/solid interface. It was found that in the presence of increasing concentration of methanol the strength of solvent-peptide and solvent-surface interactions was reduced and that consequently the interaction of the peptide with the surface increased. Increased solvent−peptide and solvent−surface interactions were responsible for a reduced interaction of the peptide with the surface in the presence of increasing concentration of glycerol. We have clearly proved that we can modulate to orientation of the peptide at the surface by changing solvent composition. Our simulations reveal that is a rather complex interplay between the reigning interacting forces between all

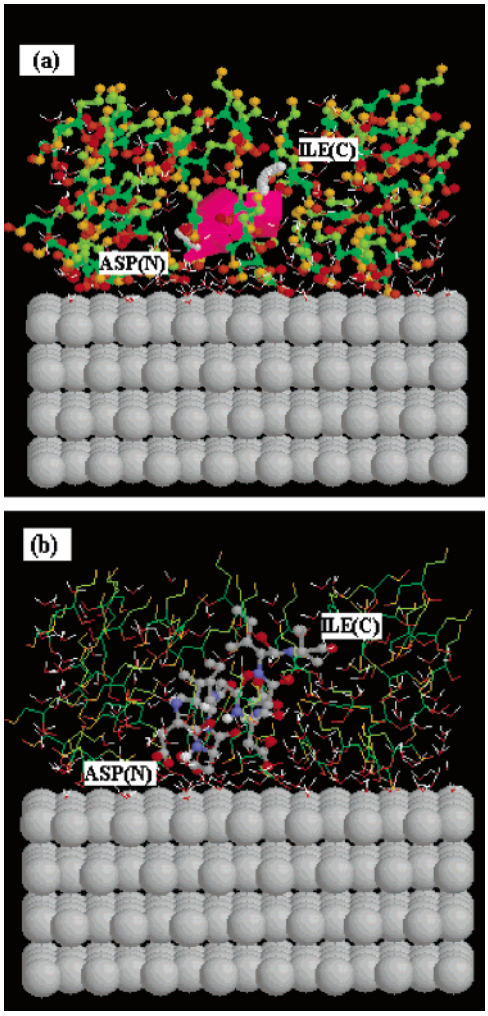

Figure 16. Visualization of the peptide at the surface in 30% glycerol (a) cartoons view of the peptide; ball-stick-view of glycerol; wireframes view of water (b) ball-and-stick view of the peptide; wireframes view of water and glycerol. Glycerol oxygen atoms are orange and yellow; Glycerol CH_2 groups are light green; Glycerol CH atoms are dark green; Glycerol hydrogen atoms are yellow and red. Water and peptide color code remains the same as in Figure 14.

the species that determines both the orientation of the peptide at the surface and its conformational stability.

Acknowledgment. This work was supported by the National Science Foundation (BES-0091542).

References and Notes

(1) Talbot, J. *Fundamentals of adsorption*; Elsevier: Paris, 1998; pp 1173−1178.
(2) Mungikar, A. A.; Forciniti, D. *ChemPhysChem* **2002**, *3*, 993−999.
(3) Gray, J. J. *Curr. Opin. Struct. Biol.* **2004**, *14*, 110−115.
(4) Hlady, V. V.; Buijs, J. *Curr. Opin. Biotechnol.* **1996**, *7*, 72−77.
(5) Nakanishi, K.; Sakiyama, T.; Imamura, K. *J. Biosci. Bioeng.* **2001**, *91*, 233−244.
(6) Siegers, C.; Biesalski, M.; Haag, R. *Chem.−Eur. J.* **2004**, *10*, 2831−2838.
(7) Lasseter, T. L.; Clare, B. H.; Abbott, N. L.; Hamers, R. J. *J. Am. Chem. Soc.* **2004**, *126*, 10220−10221.
(8) Fang, F.; Szleifer, I. *Langmuir* **2002**, *18*, 5497−5510.
(9) Lee, J. E.; Saavedra, S. S. *Langmuir* **1996**, *12*, 4025−4032.
(10) Berna, N.; Berna, P.; Oscarsson, S. *Arch. Biochem. Biophys.* **1996**, *330*, 188−192.
(11) Song, D.; Forciniti, D. *J. Colloid Interface Sci.* **2000**, *221*, 25−37.
(12) Tilton, R. D.; Robertson, C. R.; Gast, A. P. *Langmuir* **1991**, *7*, 2710−2718.
(13) Kowalczyk, D.; Slomkowski, S. *J. Bioact. Compat. Polym.* **1994**, *9*, 282−309.
(14) Burkett, S. L.; Read, M. J. *Langmuir* **2001**, *17*, 5059−5065.
(15) Mungikar, A. A.; Forciniti, D. *Biomacromolecules* **2004**, *5*, 2147−2159.
(16) Haynes, C. A.; Norde, W. *Colloids Surf. B: Biointerfaces* **1994**, *2*, 517−566.
(17) Norde, W.; Lyklema, J. *J. Biomater. Sci. Polym. Ed.* **1991**, *2*, 183−202.
(18) Darby, N. J.; Creighton, T. E. *Protein Structure*; Oxford University Press: Oxford, 1993.
(19) Kang, Y. K.; No, K. T.; Scheraga, H. A. *J. Phys. Chem.* **1996**, *100*, 15588−15598.
(20) Berendesen, H. J. C.; Postma, J. P. M.; von Gunsteren, W. F.; Hermans, J. In *Intermolecular Forces*; Pullaman, B., Ed.; Reidal: Dordrecht, The Netherlands, 1981; pp 331−342.
(21) van Gunsteren, W. F.; Billeter, S. R.; Eising, A. A.; Hünenberger, P. H.; Krüger, P.; Mark, A. E.; Scott, W. R. P.; Tironi, I. G. *Biomolecular Simulation: The GROMOS96 Manual and User Guide*; Hochschulverlag, ETH: Zürich, Switzerland, 1996.
(22) Root, L. J.; Stillinger, F. H. *J. Chem. Phys.* **1989**, *90*, 1200−1208.
(23) Allen, M. P.; Tildesley, D. J. *Computer Simulations of Liquid*; Clarendon: Oxford, U.K., 1987.
(24) Song, D.; Forciniti, D. *J. Chem. Phys.* **2001**, *115*, 8089−8100.
(25) Spohr, C. E. *J. Chem. Phys.* **1997**, *107*, 6342−6348.
(26) Yeh, Y. C.; Berkowitz, M. L. *J. Chem. Phys.* **1999**, *111*, 3155−3162.
(27) Ramachandran, G. N.; Sasisekharan, V. *Adv. Protein Chem.* **1968**, *23*, 283−438.
(28) Flory, P. J. *Statistical Mechanics of Chain Molecules*; John Wiley & Sons: New York, 1969.
(29) Sayle, R. *RasMol (Molecular visualization program) Reference Manual*, version 2.6-beta-2, 1996.
(30) Rose, G. D.; Gierasch, L. M.; Smith, J. A. *Adv. Prot. Chem.* **1985**, *37*, 1−109.
(31) Noinville, V.; Vidal-Madjar, C.; Sebille, B. *J. Phys. Chem.* **1995**, *99*, 1516−1522.
(32) Wensick, E. J. W.; Hoffman, A. C.; van Maaren, P. J.; Van Der Spool, D. *J. Chem. Phys.* **2003**, *119*, 7308−7317.
(33) Marcus, Y. *Phys. Chem. Chem. Phys.* **2000**, *2*, 4891−4896.
(34) Kvamme, B. *Phys. Chem. Chem. Phys.* **2002**, *4*, 942−948.
(35) Rosés, M.; Buhvestov, U.; Ràfols, C.; Rived, F.; Bosch, E. *J. Chem. Soc., Perkin Trans.* **1997**, *2*, 1341−1348.
(36) Gekko, K.; Timasheff, S. N. *Biochemistry* **1981**, *20*, 4677−4676.

BM050619Z